Available online at www.sciencedirect.com
ScienceDirect
Journal of Nuclear Materials 371 (2007) 90–97
journal of nuclear materials
www.elsevier.com/locate/jnucmat

An EBSD investigation on flow localization and microstructure evolution of 316L stainless steel for Gen IV reactor applications

Xianglin Wu [a], Xiao Pan [a], James C. Mabon [b], Meimei Li [c], James F. Stubbins [a,*]

[a] *Department of Nuclear, Plasma and Radiological Engineering, University of Illinois at Urbana-Champaign, 214 Nuclear Engineering Laboratory, 103 South Goodwin Avenue, Urbana, IL 61801-2984, United States*
[b] *Frederick Seitz Materials Research Laboratory, University of Illinois at Urbana-Champaign, 214 Nuclear Engineering Laboratory, 103 South Goodwin Avenue, Urbana, IL 61801-2984, United States*
[c] *Metals and Ceramics Division, Oak Ridge National Laboratory, Oak Ridge, TN 37831, United States*

Abstract

Type 316L stainless steel has been selected as a candidate structural material in a series of current accelerator driven systems and Generation IV reactor conceptual designs. The material is sensitive to irradiation damage in the temperature range of 150–400 °C: even low levels of irradiation exposure, as small as 0.1 dpa, can cause severe loss of ductility during tensile loading. This process, where the plastic flow becomes highly localized resulting in extremely low overall ductility, is referred as flow localization. The process controlling this confined flow is related to the difference between the yield and ultimate tensile strengths such that large irradiation-induced increases in the yield strength result in very limited plastic flow leading to necking after very small levels of uniform elongation. In this study, the microstructural evolution controlling flow localization is examined. It is found that twinning is an important deformation mechanism at lower temperatures since it promotes the strain hardening process. At higher temperatures, twinning becomes energetically impossible since the activation of twinning is determined by the critical twinning stress, which increases rapidly with temperature. Mechanical twinning and dislocation-based planar slip are competing mechanisms for plastic deformation.

1. Introduction

316L (LN) stainless steel has been served as a structure material for LWRs and accelerator-driven systems (ADS) for the past several decades and it is of continuing interest as candidate structural steel for Gen IV reactors conceptual designs such as sodium cooled fast reactors and lead/lead-bismuth cooled fast reactors. This reliance on 316L stainless steel is due in large part to its combination of acceptable strength and superior ductility among other assets. However, previous studies show that 316L stainless steel suffers severe radiation embrittlement in the moderate temperature range [1,2]. The tensile response is characterized by a sharp increase in yield strength, and a quick transition

* Corresponding author. Tel.: +1 217 3336474; fax: +1 217 3332906.
E-mail address: jstubbin@uiuc.edu (J.F. Stubbins).

0022-3115/$ - see front matter © 2007 Elsevier B.V. All rights reserved.
doi:10.1016/j.jnucmat.2007.05.028

to dislocation channeling or other localized flow modes at the onset of plastic deformation. This means that the ultimate tensile stress and uniform elongation would be reached very quickly once the material yields. Uniform elongation values often drop to less than 1% though the total elongations may be higher due to local ductility in the vicinity of plastic flow initiation. After exposure to irradiation, the plastic flow will be confined to very small volumes of material, as opposed to the general plastic flow in unirradiated materials. Even though there is extensive plastic flow in the small, confined regions, deformation essentially results in brittle fracture since very little energy is required to induce fracture. This process is referred as *flow localization* or *plastic instability*. Recent studies [3–5] indicate that the true stress at the onset of necking is a constant value regardless of the external irradiation level before reaching the limiting dose at which the material necks at the onset of yield. The material will fail when the true stress for the onset of plastic instability is reached. This true stress is defined as '*Critical Stress*'. This critical stress is directly correlated to the linear hardening property of materials [6] and could be obtained from the tensile property of unirradiated materials because the plastic instability limit is insensitive to irradiation dose. This value could also be found from the linear relationship between uniform elongation and yield stress in cases where full tensile curves are not available [3]. The critical stress has strong temperature dependence while the yield stress is relatively temperature insensitive. From room temperature to 200 °C, the critical stress value drops quickly and reaches a plateau thereafter. The margin between critical stress and yield strength determines the hardening capability of the material [6]. Limited studies [7–13] have been conducted to investigate the controlling mechanisms of flow localization. Planar slip and deformation twinning are believed to be the underlying microstructural mechanisms controlling plastic deformation and instability. Interrupted tensile tests were performed in this study to examine the microstructural evolution during tensile loading conditions. The electron back-scattering diffraction (EBSD) technique was applied to analyze crystallography and misorientation during tensile loading.

2. Experiment procedure

The material studied in this investigation was annealed 316L stainless steel with nominal composition given in Table 1. Interrupted tensile tests were carried out to establish the microstructural state at various levels of plastic deformation prior to the point of plastic instability, that is necking. The strain levels in the interrupted tests were determined using the hardening rate curve from the tensile test stopped at the onset of necking. Specimens at various levels of plastic strain were sliced symmetrically from the centerline and fine polished for examination with a JEOL 7000F SEM coupled with electron backscattered diffraction (ESBD) capabilities to exhibit the crystallography, crystallographic misorientation, twining and slip systems.

3. Results

The critical stress is believed to be an inherent material property and insensitive to exposed irradiation levels for face-centered cubic materials [3]. Fig. 1(a) shows the true stress–true strain curves for the EC316LN stainless steel irradiated to different dose levels and tested at room temperature [5]. It is evident that the true stress at the onset of necking is constant regardless of the irradiation levels. Since the critical stress value is invariant with irradiation exposure, it can be determined directly from unirradiated material. A shift method proposed by Byun and Farrell [5] was applied here and the result is shown as Fig. 1(b). The fact that the final plastic deformation stage leading to instability is same for materials with different irradiation exposure means that the underlying mechanism controlling flow localization is identical for all irradiation levels. Thus, it is reasonable to employ unirradiated materials to investigate the deformation mechanisms controlling flow localization.

The hardening rates and true stress versus true strain are plotted in Fig. 2 to show the strain hardening process during tensile loading at room temperature. The interrupted points are also indicated on both curves. After the initial sharp drop of strain rate, which is believed to be due to the dislocation multiplication prior to large-scale plastic deformation, the curve reaches a pseudo-plateau stage. Thereafter, the strain rates suddenly drops again and intercepts the true stress–true strain curve. This intercepting point corresponds to the onset of necking. In Fig. 2, Point A corresponds to the undeformed material; Point B represents the test interrupted at the strain at the onset of the second hardening stage after the first sharp hardening rate

Table 1
Composition for 316L stainless steel

Material	Composition (wt%)										
	C	Co	Cr	Cu	Mn	Mo	N	Ni	P	S	Si
316L SS	0.20	0.155	16.847	0.322	1.755	2.214	0.039	10.234	0.027	0.002	0.388

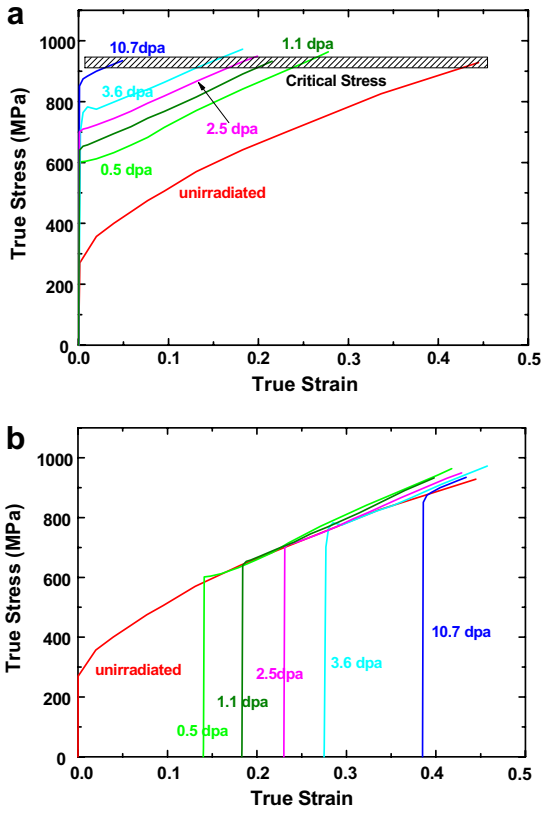

Fig. 1. EC316LN SS tested at room temperature [5]: (a), true stress–strain curves, the critical stress is labeled; and (b), the curves shifted proportional to the irradiation-induced increases in yield strength.

drop; Point C is for the test stopped at an intermediate strain and D is the onset of plastic instability.

The activation and operation of deformation twinning and planar slip systems during the tensile load are believed to be the major contributors to strain hardening. The activation of twinning is argued to be associated with the width of Shockley partial dislocations. It is more difficult for dislocations to overcome the barriers to slip when the Shockley partial is wider. The width of the Shockley partial is strongly dependent on the stacking fault energy (SFE) which is a function of material composition and temperature. For 316L stainless steel, the

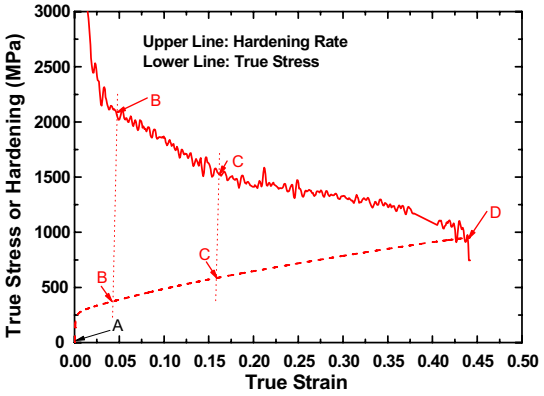

Fig. 2. The strain hardening rate (upper curve) and true stress–strain curve (lower curve) for annealed 316L SS tested at room temperature; the interrupted points are indicated.

SFE is as low as 10 mJ/m^2 [7]. At this level, the Shockley partial width is large, and then dislocation mobility is limited, inhibiting dislocation-based planar slip and promoting twinning. The trigger for the activation of twinning is believed to be determined by the critical twinning stress. In an earlier study, Byun [7] proposed a critical twinning stress expression in terms of the equivalent or uniaxial stress. The expression is revised here based on the current EBSD results as

$$\sigma_T = \frac{2\gamma_{SFE}}{b_p} \cdot \frac{1}{SF} = 4.3\frac{\gamma_{SFE}}{b_p},$$

where the average Schmidt factor (SF) is 0.465 [9]. The stacking fault energy, SFE (γ_{SFE}), values are taken from the literature [10–12]. The value of partial dislocation Burger's vector, b_p, is equal to 0.145 nm [7]. The curves for the calculated critical twinning stress also critical stress and yield strength versus test temperatures are shown in Fig. 3. The points in the figure show the relative positions of critical twinning stress with respect to the strain levels in the interrupted tests. Points A, B, C and D correspond to the ones shown in Fig. 2. The test represented by point B was stopped at the stress level lower than necessary to trigger twinning. Test C was interrupted after the activation of twinning

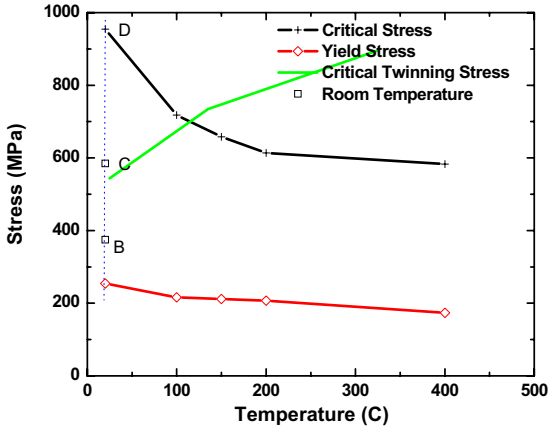

Fig. 3. Temperature dependence of critical stress, critical twinning stress and yield strength for annealed type 316L SS; the interrupted points are also indicated.

where the stress is larger than the critical twinning stress.

The microstructural evolution during tensile loading is shown in Fig. 4. The undeformed specimen has equiaxed grains and no deformation could be observed. The orientation of individual grains is uniformly distributed and no misorientations are seen, as shown in Fig. 4(a). When the specimen was strained to the onset of the second stage, Fig. 4(b), deformation is clearly evident and the grains are elongated. The rotation of single grains is becoming notable and the grains are re-orientating to the preferred orientation, i.e. ⟨1 1 0⟩ plane normal. The grey lines represent the misorientations with an angle larger than 2, but less than 10°. The deformation twinning systems have not been activated because the true stress is still smaller than the critical twinning stress. Fig. 4(c) shows the test interrupted at an intermediate strain with the true stress larger than critical twinning stress. The twins in ⟨1 1 0⟩ plane normal grains are clearly indicated as an additional deformation mechanism and the density of grains with a preferred ⟨1 1 0⟩ plane normal is greatly increased and others grains are re-orientating to this preferred orientation. Fig. 4(d) indicates the case when the material was strained to the onset of necking. The twinning systems are fully developed and, in addition, the intersection of twinning orientations is observed which is believed to be responsible for the quick drop of hardening rate and the introduction of plastic instability. In this picture, the misorientation lines are also clearly indicated.

The EBSD patterns incorporating the Schmidt factors are presented in Fig. 5. Figs. 5(a)–(d) correspond to the interrupted points A–D in Fig. 2. The left column of pictures shows the Schmidt factor distribution for each grain. The right figures are the legends; red[1] represents lower Schmidt factors and the white represents higher values.

4. Discussion

The observation of flow localization, which has been a major concern for a number of years, could be understood in the following way. First, it is noteworthy that the material exhibits a critical stress at which uniform elongation ends and necking begins. The critical stress level is independent of irradiation exposure, and appears to be an inherent material property. Second, this critical stress could be obtained from tensile tests performed on both unirradiated and irradiated material since it does not seem to depend directly on irradiation conditions. After exposure to irradiation, the material exhibits a sharp increase in yield strength which has been explained with 'barrier' hardening mechanism [14]. The post-yield hardening capability is determined by the difference between the critical stress and yield strength. The hardening rate, defined as the slope of the true stress–strain curve, exhibits a hardening rate change for each controlling deformation process. The hardening rate curve could be divided into to several stages [8]: the initial rapid decrease stage which is due to dislocation multiplication; the twinning activation and development stage; and the introduction of twin intersection which causes the onset of plastic instability. The EBSD pattern shows that the deformation process is well developed and the grains are starting to re-orient to the preferred ⟨1 1 0⟩ orientation, but no twinning could be observed. However, for the specimen strained to intermediate strain level where the stress is larger than critical twinning stress, twinning is clearly evident. Comparing these results, it can be concluded that there exists a critical twinning stress controlling the activation of twinning system as an additional deformation mechanism. Only when the stress level is larger than the critical twinning stress can the twinning system be activated. This twinning system prefers grains with ⟨1 1 0⟩ orientation and

[1] For interpretation of color in Figs. 1–5, the reader is referred to the web version of this article.

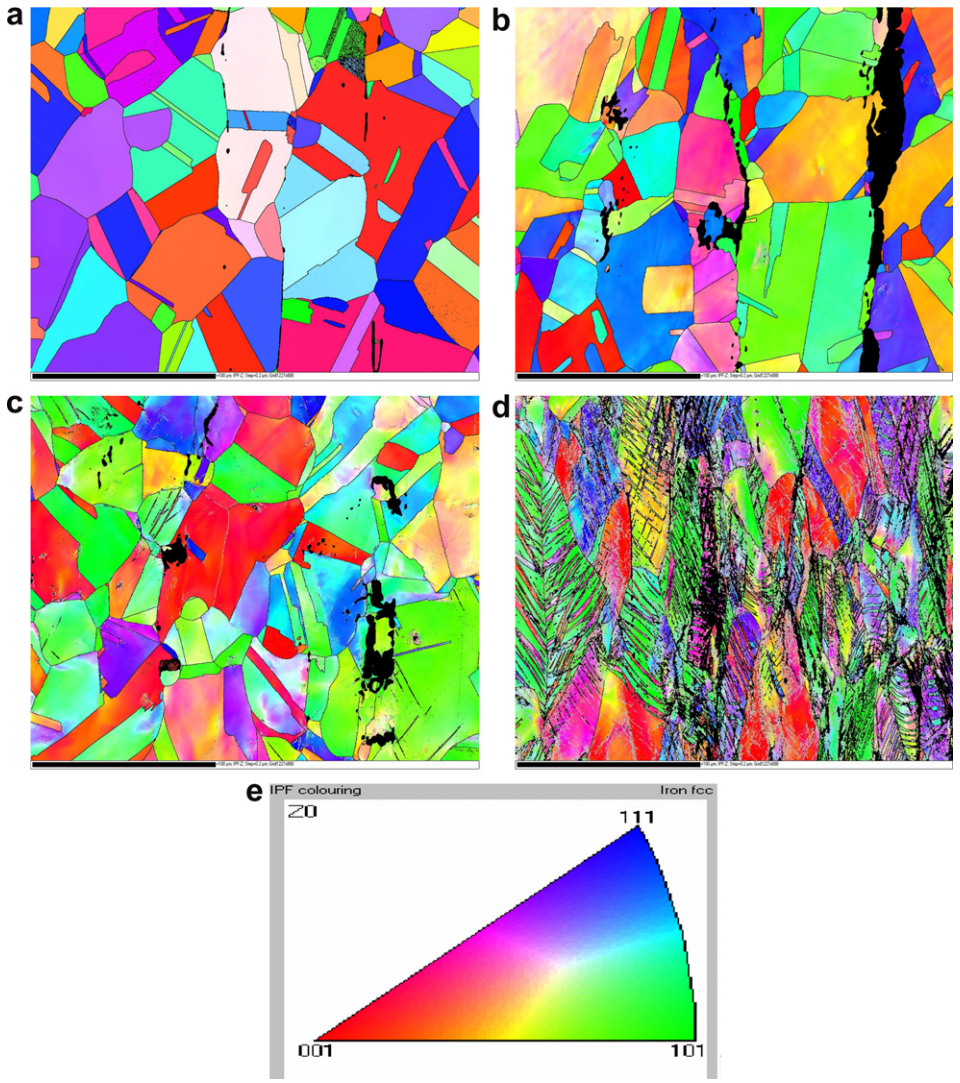

Fig. 4. SEM with EBSD pictures show the microstructure evolution, crystal orientation and misorientation for (a) undeformed, (b) interrupted at low strain level, (c) interrupted at intermediate strain level, (d) strained to uniform elongation, and (e) shows the legend for crystal orientation.

during the tensile load, the grains are re-orientating toward this orientation. The activation of the deformation twinning mechanism greatly promotes the strain hardening process and is believed to be the major factor controlling the flow localization at low temperatures.

The Schmidt factor is believed to have an important impact on the critical twinning stress and the activation of twinning. Mechanical twinning and planar slip are competing mechanism for plastic deformation. At low temperatures, the twinning system can be activated due to the relatively low critical stress to induce twinning, and this deformation mechanism acts as an additional mechanism to enhance plastic flow. Fig. 5 indicates that the twinning system can be triggered only in the grains with Schmidt factor less than about 0.485. For the grains with a higher Schmidt factor, planar slip is clearly evident from the band contrast pattern as shown in Fig. 6. This observation is consistent with the argument of competing twinning and planar slip mechanisms. The grains with Schmidt factor above 0.485 can easily satisfy the shear stress requirement for slip before the critical twinning stress is reached. After the specimen is strained to some appropriate level, where the critical twinning stress is overcome,

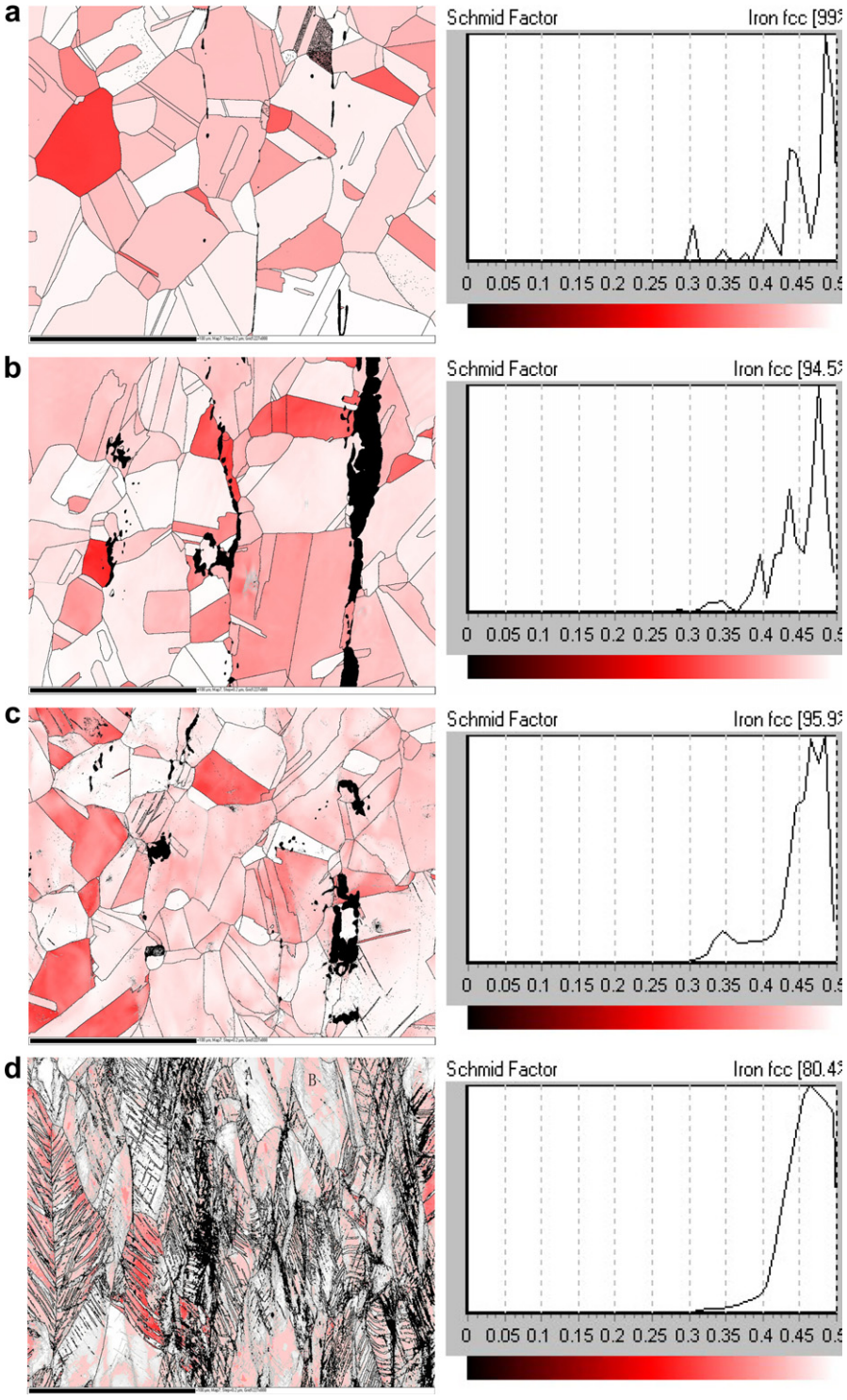

Fig. 5. Electron backscattered diffraction (EBSD) patterns incorporating with Schmidt factor for (a) undeformed, (b) interrupted at low strain level, (c) interrupted at intermediate strain level and (d) strained to uniform elongation; the left columns indicates the major differences in the amount of twinning and the right column shows the distribution of Schmidt factors.

Fig. 6. Electron backscattered diffraction (EBSD) band contrast map shows the competing mechanism between mechanical twinning and planar slip. Slip bands are clearly evident in grains A and B with high Schmidt factor.

the deformation in the grains with the most favorable slip orientations have been already dominated by dislocation-based planar slip. This can also be confirmed from band contrast map shown in Fig. 6. In the grains with high Schmidt factor, for an instance, grains A and B in Fig. 5(d) and Fig. 6, mechanical twinning is absent but slip bands are clearly evident. As the material hardens, twinning dominates the grains with preferred orientation and Schmidt factor less than 0.485. However, the grains with very high Schmidt factor have already been deformed by planar slip before twinning is triggered and twinning is no longer possible. The steep initial slope shown in Fig. 2 is the dislocation-based strain hardening behavior due to dislocation multiplication. The pseudo-plateau is due to the onset and continued activation of twinning. The twinning process permits larger ductility and increases the critical stress level. This also aids the irradiation resistance.

5. Conclusion

Analysis of the tensile response and microstructure evolution of selected series of type 316L stainless steel interrupted at various strain levels was carried out to establish the concept of critical twinning stress for activation of deformation twinning and to identify the controlling mechanisms of flow localization. The following conclusions can be drawn from the results of the study:

1. Unirradiated and irradiated type 316L stainless steels experience flow localization when the irradiation-induced hardening increases the yield strength to the level of the critical stress; the critical stress value is insensitive to irradiation level.
2. The material strain hardening process is controlled by dislocation-based hardening mechanisms and, to some extent, by mechanical twinning.
3. The activation of twinning depends on a critical twinning stress which is directly proportional to stacking fault energy and Schmidt factor; only when the stress is larger than the critical twinning stress during the plastic deformation, can the twinning be triggered as an additional plastic flow mechanism.
4. The Schmidt factor has an important impact in the activation of twinning and in the competing mechanisms of twinning and slip. In the cases examined here, some plastic, dislocation-based deformation in grains with higher Schmidt factor occurs prior to the onset of twinning, consistent with the need to reach a critical stress to activate twinning.
5. For conditions where irradiation-induced hardening occurs, the limitation in ductility is due to the margin between the elevated yield strength and the critical stress for plastic instability.

Acknowledgements

The work was supported by the US Department of Energy under grant DE-FG07-02ID14337. The authors would also like to express their appreciation to Dr Peter Kurath and Rick Rottet of Advanced Materials Testing and Evaluation Laboratory of University of Illinois at Urbana-Champaign for technical assistance. The microstructural analysis work was carried out in the Center for Microanalysis of Materials, Frederick Seitz Materials Research Laboratory, University of Illinois, which is partially supported by the US Department of Energy under grant DEFG02-91-ER45439.

References

[1] J.E. Pawel, A.F. Rowcliffe, G.E. Lucas, S.J. Zinkle, J. Nucl. Mater. 239 (1996) 126.
[2] S.A. Maloy, M.R. James, W.R. Johnson, T.S. Byun, K. Farrell, M.B. Toloczko, J. Nucl. Mater. 318 (2003) 283.
[3] X. Wu, X. Pan, M. Li, J.F. Stubbins, J. Nucl. Mater. 343 (2005) 302.

[4] X. Pan, X. Wu, M. Li, J.F. Stubbins, J. Nucl. Mater. (329–333) (2004) 1088.
[5] T.S. Byun, K. Farrell, Acta Mater. 52 (2004) 1597.
[6] X. Wu, X. Pan, M. Li, J.F. Stubbins, J. ASTM Int. 3 (1) (2006).
[7] T.S. Byun, Acta Mater. 51 (2003) 3063.
[8] E. El-Danaf, S.R. Kalidindi, R.D. Doherty, Metall. Mater. Trans. A 30A (1999) 1223.
[9] X. Wu, X. Pan, J.C. Mabon, M. Li, J.F. Stubbins, J. Nucl. Mater. 356 (2006) 70.
[10] R.M. Latanision, A.W. Ruff Jr., Metall. Trans. 2 (1971) 505.
[11] L. Remy, A. Pineau, Mater. Sci. Eng. 36 (1978) 47.
[12] F. Abrassart, Metall. Trans. 4 (1973) 2205.
[13] S.G. Song, G.T. Gray, Acta Mater. 43 (6) (1995) 2325.
[14] G.E. Lucas, J. Nucl. Mater. 206 (1993) 287.